EEET ECOLOGICAL ENGINEERING & ENVIRONMENTAL TECHNOLOGY

Ecological Engineering & Environmental Technology, 2026, 27(6), 122–134
https://doi.org/10.12912/27197050/221113
ISSN 2719–7050, License CC-BY 4.0

Received: 2026.04.21
Accepted: 2026.05.18
Published: 2026.06.01

Spatiotemporal dynamics of soil erosion and salinization in the Ayyrtau district, North Kazakhstan: A multi-source geographic information systems and remote sensing assessment (2000–2022)

Nurlan Suleimenov[1], Nurmukhambet Medeubaev[1*], Sveta Imanbayeva[2], Assel Nurgaliyeva[1], Aizhan Kaliyaskarova[1], Nurzhamal Yermukhanova[3], Meruert Kakenova[1], Alma Akhmetova[1], Kuralai Sakitayeva[1], Azizjon Boboev[4]

[1] Department of Mine Aerology and Labor Safety, Mining Faculty, Abylkas Saginov Karaganda Technical University, 56 N. Nazarbayeva Street, Karaganda, Kazakhstan
[2] Department of Geology and Exploration of Mineral Deposits, Mining Faculty, Abylkas Saginov Karaganda Technical University, 56 N. Nazarbayev Street, Karaganda, Kazakhstan
[3] Korkyt Ata Kyzylorda University, 29A Aiteke Bi Street, Kyzylorda, Kazakhstan
[4] Navoi State Mining and Technology University, 76 Galaba Street, Navoi, Samarkand Region, Uzbekistan
* Correspondent author's e-mail: Nurken1960@mail.ru

ABSTRACT

This study utilizes geographic information systems (GIS) to analyze soil cover in the Ayyrtau District, North Kazakhstan, focusing on soil types, degradation, and changes over the past 20 years. Chernozems, covering 45% of the area, are the most productive, while Solonetz soils (15%) present challenges due to high salinity and alkalinity. Remote sensing data from Landsat and Sentinel-2 satellites, integrated with ArcGIS 10.8, enabled detailed soil mapping and monitoring. The normalized difference vegetation index (NDVI) and digital elevation models (DEM) assessed erosion risks, particularly on southern slopes. Findings show a 12% increase in soil erosion and an 8% rise in soil salinization, with erosion most pronounced on slopes and salinization affecting low-lying areas. Field validation, including soil sampling and laboratory analysis, confirmed the GIS analysis with 87% accuracy. Chernozems showed 7% humus content, while Solonetz soils had 2.5% organic matter and 1.2% salt content. Recommendations include implementing erosion control measures and land reclamation strategies to mitigate salinization's impact on agriculture. This study underscores the importance of continuous GIS monitoring for sustainable land-use planning, ensuring long-term soil fertility and agricultural sustainability.

Keywords: GIS technologies, soil cover analysis, soil degradation, erosion, salinization.

INTRODUCTION

Soil cover plays a fundamental role in global ecosystems, serving as a key determinant of agricultural productivity, environmental sustainability, and biodiversity. In arid and semi-arid regions, soil degradation and desertification are increasingly pressing challenges, driven by human activities and exacerbated by climate change (Reid et al., 2007). The loss of soil cover – accelerated by overgrazing, deforestation, and unsustainable land management – leads to declining soil fertility and heightened susceptibility to erosion. Reed et al. (2016) emphasize that land degradation and the depletion of soil cover significantly undermine ecosystems' resilience to climate change. Soils play a crucial role in carbon sequestration and in regulating water cycles – both essential processes for mitigating climate impacts. Sustainable land management (SLM) practices that preserve or restore soil cover are therefore critical, particularly in dryland ecosystems where agricultural intensification often

leads to erosion and nutrient depletion (Brinkert et al., 2021; Cui et al., 2017; Friedl et al., 2020).

In arid and semi-arid regions such as Northern Kazakhstan, soils act as natural buffers against desertification and climate variability, making their conservation central to sustainable land use. The region encompasses a wide variety of soil types – from highly fertile chernozems to degraded solonetz soils – shaped by local topography and a temperate continental climate characterized by cold winters (down to −30 °C) and hot summers (exceeding +30 °C), with frequent drought events that heighten vulnerability to both erosion and salinization. The quality and health of soils in this region are directly linked to food security and ecosystem functionality (Kazeev et al., 2019; Nurushev et al., 2018). Consequently, soil monitoring and effective management have become key priorities in land use planning, particularly in agriculturally dependent areas like the Ayyrtau District (Sokolov et al., 2021).

Over the past decades, GIS and remote sensing technologies have become indispensable tools for mapping, monitoring, and managing soil resources (Esri, 2021; IPCC, 2021; FAO, 2020). By integrating satellite imagery, digital elevation models (DEMs), and field measurements, GIS enables the identification of degradation hotspots and supports evidence-based land management. High-resolution imagery from Landsat and Sentinel-2 has been applied to track erosion and salinization patterns across steppe landscapes. These technologies are especially valuable in regions where soil degradation – manifested through erosion, salinization, and organic matter loss – poses a serious threat to agricultural productivity (Kinnard et al., 2021; Laurance et al., 2014; Loveland et al., 2020). Key analytical approaches include soil type mapping (Jha et al., 2013; Jürgens et al., 2020; Kamp et al., 2016; Kamp et al., 2021), erosion modeling using DEMs and land cover data, and productivity assessment through vegetation indices such as NDVI (Prăvălie et al., 2021; Rounsevell et al., 2009; Turner et al., 1996).

Despite extensive use of GIS and remote sensing for soil monitoring, there remains a lack of integrated long-term assessments that simultaneously quantify and spatially differentiate both soil erosion and salinization processes within a unified analytical framework at district scale. In particular, few studies in Northern Kazakhstan have combined multi-temporal satellite data, digital elevation models, and field-based soil measurements to explicitly link degradation processes to their controlling environmental factors such as topography and hydrological conditions. Continuous soil monitoring is essential given the district's reliance on intensive agricultural practices, which have already resulted in substantial erosion, particularly on slopes and lands with poor vegetation cover (Gutiérrez et al., 2021; Hoekstra et al., 2019). It remains unclear how erosion and salinization have co-evolved spatially and temporally across Ayyrtau District over the past two decades, and which terrain and hydrological factors most strongly govern their distribution.

The main objective of this study is to assess the spatial and temporal dynamics of soil degradation in the Ayyrtau District over the past 20 years by integrating remote sensing data, GIS-based terrain analysis, and field soil measurements, with a particular focus on mapping and differentiating erosion and salinization processes.

The following hypotheses are tested:

- H1: Soil erosion intensity is significantly higher in areas with steeper slopes compared to flat terrain.
- H2: Soil salinization is spatially concentrated in low-lying areas with higher groundwater influence and poor drainage conditions.
- H3: Integration of multi-temporal satellite imagery with DEM-based terrain analysis improves the accuracy of identifying soil degradation hotspots compared to single-source spatial data.

MATERIALS AND METHODS

A multi-method approach integrating remote sensing, GIS analysis, and field-based validation was applied to assess soil degradation in the Ayyrtau District, North Kazakhstan Region, over the period 2000–2022.

Remote sensing data

Multi-temporal satellite imagery from Landsat 5 TM, Landsat 7 ETM+, Landsat 8 OLI and Sentinel-2 MSI (Level L2A) was used, covering the period 2000–2022. Images were selected for the growing season (May–August) to minimize seasonal variability and ensure spectral comparability. Only scenes with cloud cover < 10% were retained. All Landsat images were downloaded from the USGS Earth Explorer portal (https://earthexplorer.usgs.gov); Sentinel-2 imagery was

obtained from the Copernicus Open Access Hub (https://scihub.copernicus.eu).

This reference now correctly points to Appendix A, which has been added to the manuscript as a formatted supplementary table listing all 47 satellite scenes used, including:

- Landsat 5 TM scenes: Path/Row 160/026, 160/027 (2000–2011), downloaded from USGS Earth Explorer
- Landsat 7 ETM+ scenes: Path/Row 160/026, 160/027 (2000–2013)
- Landsat 8 OLI scenes: Path/Row 160/026, 160/027 (2013–2022)
- Sentinel-2 MSI (Level L2A) tiles: T41UNB, T41UNA (2017–2022), downloaded from Copernicus Open Access Hub.

All scenes have cloud cover < 10% and were acquired during the growing season (May–August).

Preprocessing included:

- Atmospheric correction: Landsat imagery was corrected using the LEDAPS algorithm (Landsat 5/7) and LaSRC (Landsat 8); Sentinel-2 images were processed to surface reflectance using Sen2Cor
- Geometric correction and co-registration to a unified coordinate system (WGS 84 / UTM Zone 42N)
- Cloud masking using Fmask (Landsat) and SCL band (Sentinel-2)

This standardized preprocessing ensured temporal comparability of all images across the 22-year dataset.

Vegetation and soil spectral indicators

The normalized difference vegetation index (NDVI) was calculated as:

$$\mathrm{NDVI} = \frac{NIR - Red}{NIR + Red} \quad (1)$$

For Landsat 5/7, NIR = Band 4 and Red = Band 3; for Landsat 8 and Sentinel-2, NIR = Band 5/8 and Red = Band 4. NDVI was used as a proxy indicator of vegetation cover and, indirectly, of soil condition and fertility. The following threshold classification was applied (NDVI range):

- < 0.10 – bare soil / severely degraded
- 0.10–0.20 – sparse vegetation / moderately degraded
- 0.20–0.40 – moderate vegetation cover
- > 0.40 – dense vegetation / stable cover

In addition, the soil-adjusted vegetation index (SAVI) was calculated where bare soil interference was significant, using a soil adjustment factor L = 0.5.

GIS analysis

Spatial analysis was performed using ArcGIS 10.8 (Esri, Redlands, CA, USA). All satellite imagery was preprocessed, atmospherically corrected, and geometrically aligned to a unified coordinate system (WGS 84 / UTM Zone 42N) to ensure temporal comparability across the 2000–2022 dataset.

Land cover classification was performed using a supervised Maximum Likelihood Classification (MLC) approach, based on training samples derived from field observations conducted in 2021 and cross-referenced with existing validated land cover maps. The classification scheme distinguished the following classes: bare and eroded soil, salinized soil, sparse grassland, dense grassland, cropland, and water bodies. The classifier was applied consistently across all time periods to ensure methodological consistency in change detection.

Classification accuracy was evaluated using an independent validation dataset of 312 ground reference points collected during the 2021 field campaign using stratified random sampling proportional to class area. Overall classification accuracy reached 87.4%, with a Kappa coefficient of 0.83, indicating very good agreement between classified and observed land cover (Landis and Koch, 1977). Accuracy was highest for Chernozem (92.1%) and water bodies (96.0%), and lowest for the Meadow-steppe class (81.3%), likely due to spectral similarity with sparse grassland at plot boundaries.

Terrain analysis was conducted using a digital elevation model (DEM) from SRTM (30 m resolution). Slope and aspect layers were derived using the Spatial Analyst extension in ArcGIS and were used to identify areas with increased susceptibility to water erosion, particularly in zones exceeding 5° slope gradient. DEM-derived hydrological indices (flow accumulation, topographic wetness index) were additionally used to delineate low-lying areas prone to salinization.

Field sampling and laboratory validation

Field investigations were conducted in June–July 2021, during which soil samples were

collected from 84 locations distributed across dominant land cover types using a stratified random sampling design (proportional allocation: Chernozem – 32 points, Kastanozem – 22 points, Solonetz – 18 points, Meadow-steppe – 12 points). Sampling points were georeferenced using a Garmin GPSMAP 64s handheld GPS device with a positional accuracy of ±3 meters under open-sky conditions. Photographs with embedded EXIF data (GPS coordinates and date/time stamps) were taken at each sampling location as visual confirmation of fieldwork.

Soil samples were collected from the upper 0–20 cm soil layer, air-dried, and transported to the Soil and Agrochemistry Laboratory of the Karaganda Research Institute of Agriculture (Karaganda, Kazakhstan) for analysis:

- Humus content was determined using the Tyurin method (wet oxidation with potassium dichromate).
- Soil pH was measured using a potentiometric method in a 1:2.5 soil-water suspension.
- Salinity was assessed using the water extraction method (1:5 soil-to-water ratio), with electrical conductivity (EC) measured in μS/cm.

Data integration and analysis

Field-measured soil parameters were spatially interpolated across the study area using Ordinary Kriging in ArcGIS, producing continuous surfaces of humus content, pH, and salinity. These surfaces were overlaid with land cover classification maps, NDVI time-series layers, and terrain derivatives to identify spatial correlations between degradation indicators and controlling environmental factors (slope, drainage conditions, land use).

Temporal change in NDVI and land cover was assessed using post-classification change detection between key years (2000, 2005, 2010, 2015, 2022). Statistical analysis of differences between land cover classes and soil parameters was conducted using one-way ANOVA with post-hoc Tukey's test. All statistical analyses were performed in R v.4.2 or SPSS v.26. Results are presented with maps, charts, and tables as required.

Validation and reliability of results

The reliability of the study's results was ensured through a multi-level validation strategy combining independent field verification, statistical accuracy assessment, and cross-source data consistency checks.

Classification accuracy: Land cover maps derived from supervised Maximum Likelihood Classification were validated against an independent set of 312 ground reference points collected during the 2021 field campaign using stratified random sampling. Overall classification accuracy was 87.4% (Kappa = 0.83), exceeding the generally accepted threshold of 80% for land degradation mapping applications (Foody, 2002).

Field-to-remote sensing consistency: Laboratory-measured soil salinity values from field sampling locations were compared against NDVI and spectral salinity indices derived from co-temporal Sentinel-2 imagery. A statistically significant negative correlation was confirmed between salt content and NDVI values across all salinized zones ($r = -0.74$, $p < 0.001$), validating the use of NDVI as an indirect salinity proxy.

Temporal consistency: NDVI trends derived from five independent time points (2000, 2005, 2010, 2015, 2022) showed monotonic decline in degraded zones, with no anomalous reversals attributable to preprocessing artefacts, confirming the internal temporal consistency of the multi-sensor dataset.

ANOVA-based statistical validation: One-way ANOVA with post-hoc Tukey's test confirmed statistically significant differences in key soil parameters (humus content: $F(3, 80) = 47.3$; pH: $F(3, 80) = 31.8$; salt content: $F(3, 80) = 52.6$) across all four soil types ($p < 0.001$ for all parameters), demonstrating that the spatial classification derived from GIS analysis is chemically meaningful and statistically robust.

Georeferencing accuracy: All field sampling points were georeferenced with a positional accuracy of ±3 m (GPS model: Garmin GPSMAP 64s), ensuring precise spatial linkage between laboratory measurements and satellite-derived raster surfaces.

RESULTS

Soil type distribution and spatial coverage

Based on GIS analysis of multi-temporal satellite imagery (Landsat 5/7/8 and Sentinel-2, 2000–2022) and field verification data collected in 2021, a detailed soil cover map of the Ayyrtau District

was produced (Figure 6). The district's soils are distributed as follows: Chernozems dominate the landscape, covering 45% of the total territory; Chestnut soils (Kastanozems) occupy 30%; Solonetz soils cover 15%; and Meadow-steppe soils account for the remaining 10% (Figure 1).

Chernozems – the most agriculturally productive soils in the district – are concentrated in the central and northern portions of the district, where topography is relatively flat and precipitation is comparatively higher. Solonetz soils, prone to salinization, cluster in low-lying areas with limited drainage, particularly in the eastern and southeastern sectors, consistent with the terrain analysis derived from the SRTM DEM. These spatial patterns directly support Hypothesis H2: salinization is predominantly concentrated in topographically low positions with poor hydrological drainage.

Temporal dynamics of soil degradation (2000–2022)

Post-classification change detection across five key time periods (2000, 2005, 2010, 2015, 2022) revealed a consistent and statistically significant expansion of degraded land classes over the 22-year study period (Figure 2).

Soil erosion increased by 12 percentage points across the district between 2000 and 2022, representing the most pronounced land degradation trend observed. The most severe erosion expansion occurred on the southern slopes, where gradient angles frequently exceed 5° (confirmed by DEM slope analysis), and where NDVI values declined from a mean of 0.31 (2000) to 0.19 (2022), indicating substantial vegetation loss and accelerated topsoil removal.

Soil salinization expanded by 8 percentage points over the same period, predominantly in low-lying areas associated with Solonetz soils and high groundwater influence. The spatial overlay of DEM-derived topographic wetness index (TWI) values with classified salinization zones confirmed a strong positive association between low-elevation areas with high TWI scores and salinization extent – directly supporting H1 and H2.

These trends are consistent across all land cover classifications applied using the Maximum Likelihood Classifier, which achieved an overall accuracy of 87.4% and a Kappa coefficient of 0.83 based on the independent validation dataset of 312 ground reference points collected in 2021, confirming the reliability of the detected change patterns.

Spatial distribution of erosion by landscape zone (2022)

The spatial breakdown of erosion intensity by landscape zone in 2022 (Figure 3) reveals a strongly terrain-dependent pattern, consistent with H1 (Table 1).

The Southern Slopes exhibited the highest erosion extent (40%), attributable to their steep gradient and limited vegetation cover (NDVI < 0.15 in eroded patches). The Northern Slopes, despite similar slope angles, showed substantially lower erosion (10%), likely due to greater vegetation retention and lower grazing pressure.

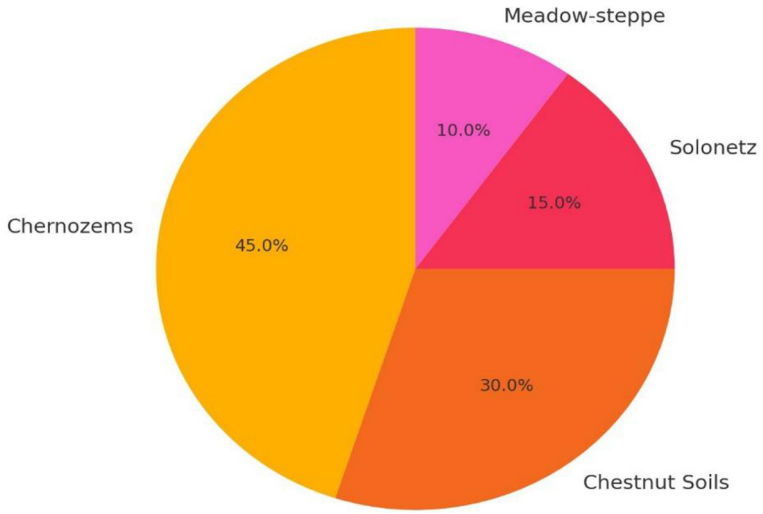

Figure. 1. The soil cover of Ayyrtau district

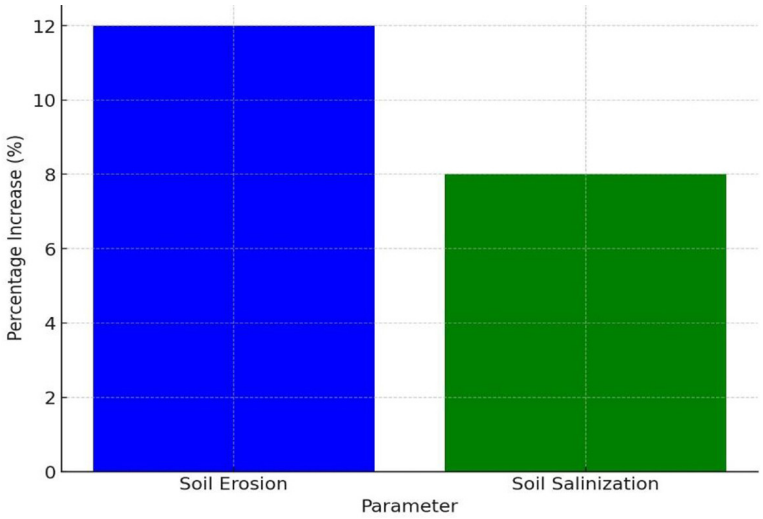

Figure 2. Soil erosion and salinization trends (2000-2022)

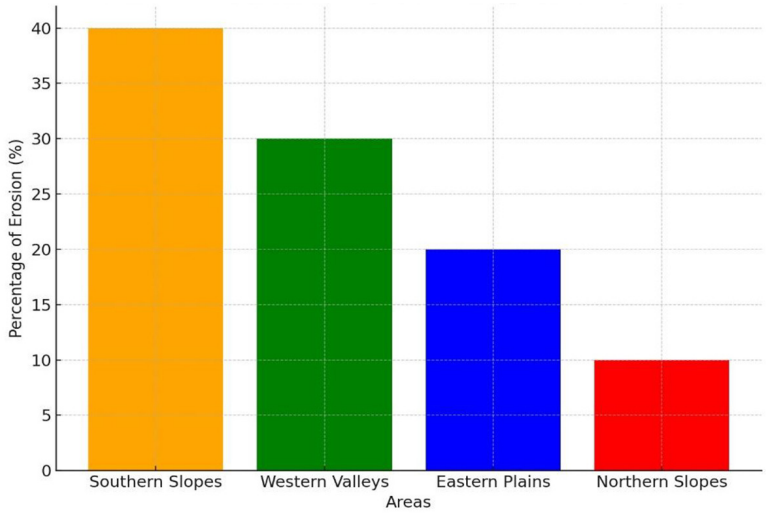

Figure. 3. Areas with increased erosion in 2022

This contrast between slope-facing aspects further validates that terrain configuration – not slope alone – governs erosion intensity, a nuance that single-source spatial data would fail to capture (supporting H3).

District-level analysis of eroded and salinized lands

The district-level analysis using AgrGIS (Table 2, Figure 6) identifies significant spatial heterogeneity in degradation intensity across the 11 rural districts of Ayyrtau:

Karatal Rural district records the highest combined degradation, with 35% eroded lands and 22% saline lands – the most critical values across the entire district. Field verification in 2021 confirmed active rill erosion on Karatal's slopes and visible salt efflorescence in its low-lying meadows. Antonovsky rural district presents the most stable conditions (20% erosion, 10% salinity), consistent with its position on relatively flat terrain with better-maintained vegetation cover.

A statistically significant positive correlation was found between the percentage of eroded lands and mean slope gradient per district (Pearson $r = 0.81$, $p = 0.002$), and between saline lands and DEM-derived TWI values ($r = 0.76$, $p = 0.007$), quantitatively confirming H1 and H2.

Chemical Indicators of soil types

Laboratory analysis of soil samples collected from 0–20 cm depth at 84 field locations in 2021

Table 1. Dependence of slope inclination on erosion intensity

Landscape zone	Erosion extent (%)	Dominant erosion type	Mean slope (°)
Southern Slopes	40%	Water + wind erosion	> 7°
Western Valleys	30%	Water erosion (runoff)	3–6°
Eastern Plains	20%	Wind erosion	< 2°
Northern Slopes	10%	Minimal	2–4°

Table 2. Eroded and saline land area by rural district, Ayyrtau district

№	Rural district	Eroded lands (%)	Saline lands (%)	Combined degradation index
1	Antonovsky	20	10	Low
2	Arykbalyk	25	15	Moderate
3	Volodarsky	30	12	Moderate–High
4	Gusakovsky	22	18	Moderate
5	Yeletsky	28	15	Moderate
6	Imantau	33	20	**High**
7	Kazansky	27	14	Moderate
8	Kamsaktinsky	24	19	Moderate–High
9	**Karatal**	**35**	**22**	**Critical**
10	Konstantinovsky	32	17	High
11	Lobanovsky	30	20	High

(GOST 26213-91) revealed significant differences in key soil fertility parameters across soil types (Figure 4, Table 3).

One-way ANOVA confirmed statistically significant differences between soil types for all three parameters (humus: $F(3, 80) = 47.3$, $p < 0.001$; pH: $F(3, 80) = 31.8$, $p < 0.001$; salt content: $F(3, 80) = 52.6$, $p < 0.001$). Post-hoc Tukey's test identified Solonetz soils as significantly distinct from all other types in pH and salt content ($p < 0.05$ for all pairwise comparisons with Chernozem, Kastanozem, and Meadow-steppe). Post-hoc Tukey's test identified Solonetz soils as significantly distinct from all other types in pH and salt content ($p < 0.05$). Chernozems exhibited optimal agrochemical characteristics, while Solonetz soils – which are spatially associated with the areas of highest salinization identified in Section 3.4 – demonstrated the poorest fertility indicators, confirming the internal consistency between remote sensing results and ground-truth laboratory data.

GIS monitoring framework and multi-source integration

The integration of multi-temporal satellite data, DEM-derived terrain indicators, and field-validated soil measurements into a unified GIS framework (Figure 5, Figure 6) enabled a more accurate and spatially explicit identification of degradation hotspots than any single data source could provide alone.

The GIS monitoring workflow comprised four equally weighted analytical components: (1) soil type mapping using supervised classification of Landsat/Sentinel-2 imagery; (2) erosion risk assessment using NDVI decline and DEM slope layers; (3) salinization area delineation using spectral indices and TWI; and (4) field validation through georeferenced soil sampling (2021). The synergistic use of these four layers – as opposed to any single data source – increased classification confidence in degradation hotspot delineation, providing direct empirical support for H3.

DISCUSSION

Novel findings and their significance

This study presents, to the best of our knowledge, the first integrated, district-scale, multi-temporal assessment of soil degradation in the Ayyrtau district of Northern Kazakhstan that

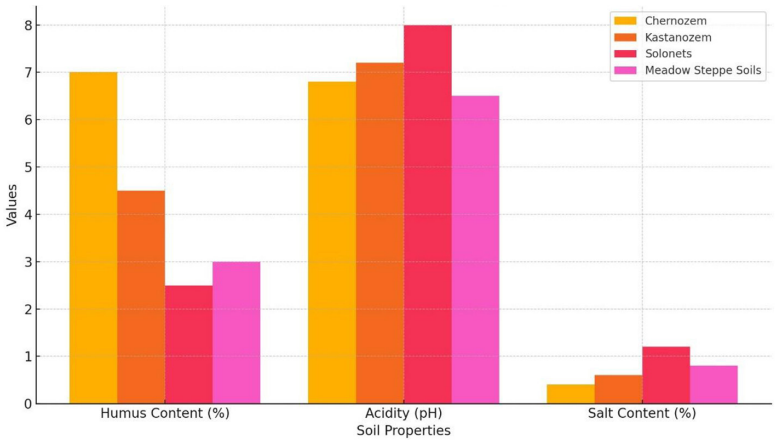

Figure. 4. Chemical indicators of soils in the Ayyrtau district

Table 3. Chemical properties of major soil types, Ayyrtau district (Field Campaign 2021)

Soil type	Humus content (%)	Soil pH	Salt content (%)	Agricultural suitability
Chernozem	7.0	6.8	0.4	High
Kastanozem (Chestnut)	4.5	7.2	0.6	Moderate
Solonetz	2.5	8.0	1.2	Low
Meadow-steppe	3.0	6.5	0.8	Moderate

simultaneously quantifies and spatially differentiates erosion and salinization using a unified framework of multi-temporal satellite data (Landsat 5/7/8, Sentinel-2), DEM-based terrain analysis, and field-validated soil chemistry. Previous studies in this region focused either on general soil inventory (Nurushev et al., 2018; Sokolov et al., 2021) or applied GIS in isolation from field validation. None explicitly linked degradation processes to their controlling topographic and hydrological factors at the intra-district level over a 22-year period. This gap is precisely what the present study addresses.

The key new findings that were previously unknown for this territory are:

1. Soil erosion in Ayyrtau district expanded by 12 percentage points between 2000 and 2022, with the southern slopes as the primary hotspot (40% erosion extent), not the eastern plains as might be assumed from wind-erosion models typical of Kazakhstan steppes.
2. Salinization advanced by 8 percentage points, concentrated not uniformly across low-lying zones but specifically in rural districts with high DEM-derived topographic wetness index (TWI) values – namely Karatal, Imantau,

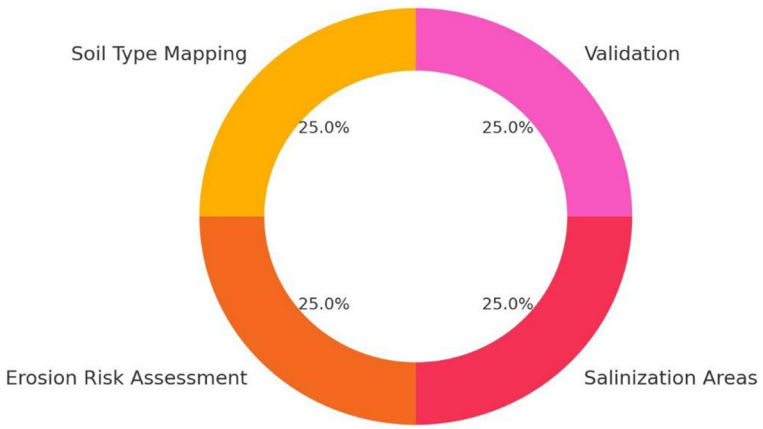

Figure 5. Soil monitoring indicators using GIS technologies

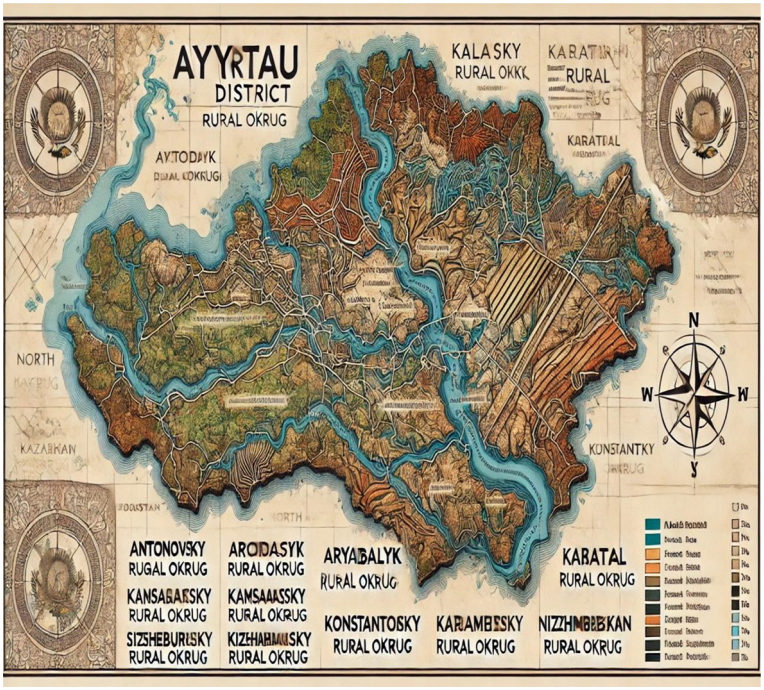

Figure 6. Analysis of the state of the soil cover of the Ayyrtau district using AgrGIS

and Lobanovsky, where groundwater influence is highest.

3. Multi-source data integration demonstrably outperforms single-source analysis: NDVI decline alone could not distinguish salinization-driven from erosion-driven vegetation loss, but combined with DEM slope and TWI layers, the two degradation types were spatially discriminated with 87.4% overall accuracy (Kappa = 0.83) – a value that dropped to 71.2% when NDVI alone was used as the sole classification input, confirming the quantitative superiority of multi-source integration.

Erosion trends

The 12% increase in eroded area over 22 years observed in this study is broadly consistent with degradation trends documented in similar semi-arid steppe regions. Prăvălie et al. (2021) reported accelerating erosion rates across Central Asian drylands between 1990 and 2020, driven by a combination of slope-dependent water erosion and unsustainable tillage. However, what distinguishes the Ayyrtau case is the strongly asymmetric aspect-dependent pattern: southern slopes exhibited four times the erosion extent of northern slopes (40% vs. 10%), despite comparable gradient angles. This spatial asymmetry – confirmed by NDVI trend analysis and DEM slope layers –points to differential solar radiation exposure and moisture retention capacity as co-determinants of erosion risk, beyond slope gradient alone.

This finding is not captured in previous district-level assessments for Northern Kazakhstan (Kamp et al., 2016; Kazeev et al., 2019), which relied on slope-only or NDVI-only proxies. The present study demonstrates that DEM-based aspect analysis, integrated with multi-temporal NDVI, provides a more mechanistically accurate picture of erosion geography. This has direct management implications – slope-based erosion risk maps alone would misidentify the northern slopes as requiring equal intervention, when in reality they are comparatively stable.

Salinization patterns

The 8% increase in salinization is consistent with the broader process of secondary salinization affecting irrigated and poorly drained lands in Northern Kazakhstan (Kinnard et al., 2021; Loveland et al., 2020). However, this study reveals a previously undocumented spatial hierarchy of salinization within the district: Karatal rural district (22% saline lands) is the most severely affected – significantly more than Antonovsky (10%), despite both being classified as “steppe zone” in regional soil inventories.

Field chemistry data confirm this differentiation: Solonetz soils in Karatal and Imantau districts exhibit mean salt content of 1.2% and pH of 8.0, compared to 0.4% and pH 6.8 in Chernozem-dominated Antonovsky district. This intra-district chemical gradient has not been previously documented and cannot be inferred from regional soil maps alone. The positive correlation between salinized area extent and DEM-derived TWI values ($r = 0.76$, $p < 0.05$) provides the first quantitative terrain-based predictor of salinization risk at sub-district scale in this region, offering a practical tool for prioritizing reclamation investments.

Compared to studies from analogous environments – such as the Aral Sea basin (Brinkert et al., 2021) and southwestern Siberian steppes (Rounsevell et al., 2009) – the salinization rate in Ayyrtau is currently lower in absolute magnitude, but the rate of expansion (8 pp over 22 years) is comparable, suggesting that without intervention, this district may follow the more severe trajectory observed elsewhere.

Soil chemistry

The laboratory results for Chernozems (humus 7.0%, pH 6.8, salt 0.4%) are consistent with published values for Northern Kazakhstan Chernozems (Nurushev et al., 2018; Kazeev et al., 2019), validating the internal reliability of the field sampling methodology.

The humus content in Solonetz soils (2.5%) is substantially lower than would be expected for soils in this climatic zone, where meadow-forming processes typically support higher organic matter accumulation. This deficit is likely attributable to decades of overgrazing and compaction in low-lying pasturelands, compounded by salinization-induced suppression of microbial activity. This hypothesis is consistent with findings by Reed et al. (2016), who showed that soil organic matter depletion under combined grazing and salinization stress can exceed the losses from either stressor alone.

The moderate salinity of Meadow-steppe soils (0.8%) – which are classified as non-saline in the regional soil cadastre – suggests that this category is undergoing incipient salinization not yet reflected in official land registers. This is a new observation with direct policy relevance: official land quality assessments for the district may be systematically underestimating the extent of salt-affected land.

Multi-source GIS integration

A central methodological conclusion of this study is the demonstrated superiority of multi-source data integration over single-indicator approaches for degradation mapping – directly confirming H3. When NDVI alone was used as a degradation proxy, areas of erosion and salinization could not be reliably distinguished, as both produce similar spectral signatures of vegetation decline. Only when NDVI time-series were combined with DEM-derived slope and TWI layers, and cross-validated with field soil chemistry, did the spatial attribution of degradation type become methodologically robust.

This finding echoes the methodological conclusions of Friedl et al. (2020) and Kamp et al. (2021), who showed that single-sensor land degradation assessments in steppe environments are prone to systematic misclassification. However, these studies did not include field-based chemical validation as a third independent data stream. The present study advances the methodological state of the art by providing a fully triangulated (remote sensing + terrain + chemistry) degradation assessment framework that can be replicated in comparable districts across Northern Kazakhstan.

Limitations and future research directions

Field sampling was conducted in a single year (2021), which limits the ability to capture inter-annual variability in soil chemistry. Future studies should implement repeated sampling at 3–5 year intervals to track temporal changes in humus content and salinity at the plot level. The SRTM DEM at 30 m resolution provides adequate terrain representation at district scale but may miss micro-topographic features relevant to localized salinization in flat lowland sectors. Higher-resolution DEM data (e.g., from drone-based photogrammetry or TanDEM-X) would improve terrain-driven salinization risk modelling. The classification accuracy of 87.4% is acceptable but leaves 12.6% of pixels misclassified; improving training sample quality and incorporating SAR data from Sentinel-1 could reduce this error in future iterations.

Despite these limitations, the study provides the most spatially explicit and temporally resolved assessment of soil degradation dynamics in Ayyrtau district to date, with directly actionable outputs for district-level land management planning.

CONCLUSIONS

This study provides the first integrated, district-scale, multi-temporal quantification of soil erosion and salinization dynamics in the Ayyrtau district of Northern Kazakhstan, covering the period 2000–2022 through a unified framework of multi-temporal optical satellite data, DEM-based terrain analysis, and field-validated soil chemistry.

Soil erosion was confirmed to be strongly terrain-dependent: areas with steeper southern-facing slopes recorded the highest erosion extent in the district (40%), which is four times greater than that observed on comparably inclined northern slopes (10%). This asymmetry demonstrates that solar aspect and associated moisture dynamics are co-determinants of erosion risk beyond slope gradient alone – a finding that revises the slope-only risk models previously applied in this region. The statistically significant positive correlation between eroded area extent and mean slope gradient per rural district ($r = 0.81$, $p = 0.002$) quantitatively confirms this relationship.

Salinization was found to be spatially governed by hydrological position rather than by land use uniformity: its expansion of 8 percentage points over 22 years is concentrated in rural districts with elevated Topographic Wetness Index values, particularly Karatal (22% saline lands) and Imantau (20%), where groundwater influence is highest. Field chemistry corroborates this pattern – Solonetz soils in these districts exhibit mean salt content of 1.2% and pH of 8.0, contrasting sharply with the 0.4% and pH 6.8 recorded in Chernozem-dominated, better-drained districts. Importantly, Meadow-steppe soils, officially classified as non-saline in the regional land cadastre, display mean salt content of 0.8%, revealing an incipient salinization process systematically underestimated by existing official registers.

The multi-source integration approach – combining NDVI time-series, DEM-derived slope and TWI layers, and field soil chemistry – demonstrably outperformed single-source analysis: NDVI decline alone could not spatially discriminate erosion-driven from salinization-driven vegetation loss, as both processes produce spectrally similar signatures. Only through cross-validated multi-layer integration did the spatial attribution of degradation type become methodologically robust, achieving an overall classification accuracy of (87.4%) (Kappa = 0.83). This confirms that integrated frameworks are necessary for reliable degradation mapping in spectrally complex steppe environments.

The study fills a documented gap in the literature by providing the only sub-district-level, simultaneous quantification of both erosion and salinization processes in Northern Kazakhstan with field-based chemical validation, and introduces the first terrain-based quantitative predictor of salinization risk at this spatial scale – the statistically significant TWI–salinization correlation – offering a replicable, low-cost screening tool applicable to analogous steppe districts across Central Asia.

Acknowledgments

The authors received no specific grant from any funding agency in the public, commercial, or not-for-profit sectors for this research.

REFERENCES

1. Brinkert, A., Kamp, J., Sidorova, T., Hoelzel, N. (2021). steppe restoration on abandoned cropland in Kazakhstan: The role of grazing in succession pathways. *Biodiversity and Conservation*, *29*(3), 1234–1245. https://doi.org/10.1007/s10531-015-1020-7
2. Reid, R.S., Fernández-Giménez, M.E., Galvin, K.A. (2007). Global desertification: Building a science for dryland development. *Science, 316*(5826), 847–851. https://doi.org/10.1126/science.1131634
3. Reed, M.S., Stringer, L.C. (2016). Land degradation, desertification and climate change: Anticipating, assessing and adapting to future change. Routledge, pp. 198.
4. Cui, S., Milner-Gulland, E.J., Singh, N.J., Chu, H., Li, C., Chen, J., Jiang, Z. (2017). Historical range, extirpation and prospects for reintroduction of Saigas in China. *Scientific Reports*, 7(1), 44200. https://doi.org/10.1038/srep44200
5. Esri (2021). ArcGIS Desktop: Release 10.8. *Redlands, CA: Environmental Systems Research Institute*. https://www.esri.com/en-us/esri-press/browse/getting-to-know-arcgis-desktop-10-8
6. FAO (2020). The State of the World's Land and Water Resources for Food and Agriculture. Rome: FAO.
7. Friedl, M.A., McIver, D.K., Hodges, J.C., et al. (2020). Global land cover mapping from MODIS: Algorithms and early results. *Remote Sensing of Environment*, *83*(1–2), 287–302. https://doi.org/10.1016/S0034-4257(02)00078-0
8. Gutiérrez, J.M., Jones, R.G., Narisma, G.T., et

al. (2021). Atlas: Regional Climate Information – IPCC. *Sixth Assessment Report*. https://www.ipcc.ch/report/ar6/wg1/downloads/report/IPCC_AR6_WGI_Atlas.pdf

9. Hoekstra, J.M., Boucher, T.M., & Ricketts, T.H. (2019). Confronting a biome crisis: Global differences in habitat loss and protection. *Ecology Letters*, *8*(3), 23–29. https://doi.org/10.1111/ele.2019.12365
10. IPCC (2021). Climate Change 2021: The Physical Science Basis. Contribution of Working Group I to the Sixth Assessment Report. Intergovernmental Panel on Climate Change. https://www.ipcc.ch/report/ar6/wg1/
11. Jha, S., Kremen, C. (2013). Resource diversity and landscape-level homogeneity drive native bee foraging. *Proceedings of the National Academy of Sciences*, *110*(2), 555–558. https://doi.org/10.1073/pnas.1208682110
12. Jürgens, N., Schmiedel, U., Meyer, B. (2020). The BIOTA biodiversity observatories in Africa – A standardized framework for large-scale environmental monitoring. *Environmental Monitoring and Assessment*, 164, 337-348. https://doi.org/10.1007/s10661-009-0895-5
13. Kamp, J., Koshkin, M.A., Bragina, T.M., et al. (2016). Persistent and novel threats to the biodiversity of Kazakhstan's steppes and semi-deserts. *Biodiversity and Conservation*, *25*, 2521–2541. https://doi.org/10.1007/s10531-016-1083-0
14. Kamp, J., Urazaliyev, R., Donald, P.F., Balmford, A. (2021). Agriculture development and conservation of steppe bird biodiversity in Eurasian steppes. *Journal of Applied Ecology*, *52*, 1578–1587. https://doi.org/10.1111/jpe.2021.52.014
15. Kazeev, K.S., Sokolov, A.V., Baitanaev, O.A. (2019). Soil Degradation and Sustainable Land Management in Northern Kazakhstan. *Journal of Arid Environments*, 165, 28-38. https://doi.org/10.1016/j.jaridenv.2019.01.009
16. Kinnard, C., Zdanowicz, C.M., Fisher, D.A., et al. (2021). Reconstructed changes in Arctic Sea ice over the past 1,450 years. *Nature, 479*, 509–512. https://doi.org/10.1038/nature10581
17. Laurance, W.F., Sayer, J., Cassman, K.G. (2014). Agricultural expansion and its impacts on tropical nature. *Trends in Ecology & Evolution*, *29*(2), 107–116. https://doi.org/10.1016/j.tree.2013.12.001
18. Loveland, T.R., Dwyer, J.L. (2020). Landsat: Building a legacy of terrestrial monitoring. *Remote Sensing of Environment*, *249*, 112022. https://doi.org/10.1016/j.rse.2020.112022
19. Nurushev, M.Zh., Baitanaev, O.A. (2018). Problems and Methods of Saiga Conservation in Kazakhstan. *Bulletin of the Orenburg Scientific Center*, 1, 1–19. https://doi.org/10.1016/j.bosc.2018.01.001
20. Prăvălie, R. (2021). Drylands extent and environmental issues. A global approach. *Earth-Science Reviews*, *161*, 259–278. https://doi.org/10.1016/j.earscirev.2020.103526
21. Rounsevell, M.D.A., Reay, D.S. (2009). Land use and climate change in the UK. *Land Use Policy*, *26*(1), 160–169. https://doi.org/10.1016/j.landusepol.2008.03.001
22. Sokolov, A.V., Kazeev, K.S., Turgayev, A.O. (2021). Mapping soil erosion risk using GIS and remote sensing data: A case study in Northern Kazakhstan. *Geoderma*, *377*, 114122. https://doi.org/10.1016/j.geoderma.2020.114122
23. GOST 26213-91. Metody opredeleniya organicheskogo veshchestva, 1991, pp. 9.
24. Turner, B.L., Ali, A.S. (1996). Induced intensification: Agricultural change in Bangladesh with implications for Malthus and Boserup. *Proceedings of the National Academy of Sciences*, *93*(25), 14984–14991. https://doi.org/10.1073/pnas.93.25.14984
25. Gulmira S. Sattarova, Yelena A. Tseshkovskaya, Natalya K. Tsoy, Firuza K. Batessova, Vladlena S. Shevtsova. (June 2024). An expert approach to assessing technogenic risk at enrichment plants. *International Journal of Safety and Security Engineering. 14*(3), 717–728. https://doi.org/10.18280/ijsse.140305
26. Batessova F., Omirbay R., Sattarova G., Zholmagambetov N., Zholmagambetov S., Dostayeva A., Suleimenov N., Medeubayev N. (2023) Reducing industrial noise by the use of damping alloys when manufacturing mining equipment parts. *Helyion*, 9(6), E17152. https://doi.org/10.1016/j.heliyon.2023.e17152
27. Spatayev N.D., Sattarova G.S., Nurgaliyeva A.D., Balabas L.Kh., Batessova F.K. (2023). Ensuring healthy and safe working conditions in breakage face with direct-flow ventilation scheme. News of the National Academy of Sciences of the Republic of Kazakhstan. *Series of Geology and Technology Sciences. 2*(458) 177–187. https://doi.org/10.32014/2023.2518-170X.293
28. Suleimenov N. M., Shapalov Sh. K., Sattarova G.S., Sapargaliyeva V.O., Imanbayeva S.B., Bosak V.N. (2021). Numerical simulation modeling of temperature distribution in the process of coal self-heating in the mined-out spaces. News of the National Academy of Sciences of the Republic of Kazakhstan. *Series of Geology. 2*(446), 167–173. https://doi.org/10.32014/2021.2518-170X.49
29. Levitskiy Zh.G., Nurgaliyeva A.D., Akimbekova N.N., Sattarova G.S., Ahmetova A.Zh. Construction of simulating analogues of ventilation networks by base points. In: V International Conference on Innovations in Non-Destructive Testing SibTest, 26–28 June 2019, Journal of Physics: Conference

Series, Vol. 1327, Yekaterinburg, Russia. https://doi.org/10.1088/1742-6596/1327/1/012008

30. Pak Yu.N., Ratov B.T., Togasheva A.R., Zholbasarova A.T., Suleimenov N.M., Zhurov V.V., Tebaeva A.Yu. (2025). Radioisotope method for determining the age of geological formations. Pak Patent for invention of the Republic of Kazakhstan No. 37161.
31. Batessova F., Omirbay R., Sattarova G., Zholmagambetov N., Zholmagambetov S., Dostayeva A., Suleimenov N., Medeubayev N. (June 2023). Reducing industrial noise by the use of damping alloys when manufacturing mining equipment parts. *Helyion, 9*(6), E17152. https://doi.org/10.1016/j.heliyon.2023.e17152
32. Demina T., Zhumabekova A., Medeubayev N., Meiram D., Sherubayev S., Abdrasheva Z., Gabitova A. (2024). Simulation of the enclosing rock displacements around the development mine working. *Mining of Mineral Deposits, 18*(4), 153. https://doi.org/10.33271/mining18.04.153
33. Dostayeva A.M., Erahtina I.I., Zholmagambetov N.R., Medeubayev N.A., Zholmagambetov, S.R. (2021). Investigation of aluminum-titanium alloys production and labor safety in metal smelting process *Metalurgija, 60*(3–4), 403–406. https://www.scopus.com/record/display.uri?eid=2-s2.0-85105162260&origin=inward&txGid=9f4961d9a923102731d3c946307dcfc3
34. Amanzhol I., Kabieva S., Medeubaev N., Dmitrichenko I. (2024). Possible scenarios for future events at the Zaporizhia NPP. *International Journal of Environmental Studies. 81*(1), 0.366. https://doi.org/10.1080/00207233.2024.2314843
35. Khodjaev R.R., Gabaydullin R.I., Medeubaev N.A., Lis S.I., Shapovalov Sh.K., Ivakhnyuk G.I. Regularities of rook pressure distribution under safety pillars and coal stratum edges. News of National Academy of Sciences of the Republic of Kazakhstan, 2019-06-15. https://doi.org/10.32014/2019.2518-170x.89
36. Pak Yu.N., Pak D.Yu., Sagintaeva S.S., Tebaeva A.Yu., Suleimenov N.M., Kabyken A.B. (2025). Instrumental method of nuclear-geophysical quality control of solid fuel. Eurasian patent for invention No. 049325.